CHEMISTRY
A EUROPEAN JOURNAL

DOI: 10.1002/chem.200500796

Atropisomeric Discrimination in New Ru^{II} Complexes Containing the C_2-Symmetric Didentate Chiral Phenyl-1,2-bisoxazolinic Ligand

Xavier Sala,[a] Elena Plantalech,[a] Isabel Romero,[a] Montserrat Rodríguez,*[a] Antoni Llobet,*[b] Albert Poater,[c] Miquel Duran,[c] Miquel Solà,*[c] Susanna Jansat,[d] Montserrat Gómez,[d] Teodor Parella,[e] Helen Stoeckli-Evans,[f] and Jordi Benet-Buchholz[g]

Abstract: A new family of Ru^{II} complexes containing the tridentate meridional 2,2′:6′,2″-terpyridine (trpy) ligand, a C_2-symmetric didentate chiral oxazolinic ligand 1,2-bis[4′-alkyl-4′,5′-dihydro-2′-oxazolyl]benzene (Phbox-R, R = Et or *i*Pr), and a monodentate ligand, of general formula $[Ru(Y)(trpy)(Phbox\text{-}R)]^{n+}$ (Y = Cl, H_2O, py, MeCN, or 2-OH-py (2-hydroxypyridine)) have been prepared and thoroughly characterized. In the solid state the complexes have been characterized by IR spectroscopy and by X-ray diffraction analysis in two cases. In solution, UV/Vis, cyclic voltammetry (CV), and one-dimensional (1D) and two-dimensional (2D) NMR spectroscopy techniques have been used. We have also performed density functional theory (DFT) calculations with these complexes to interpret and complement experimental results. The oxazolinic ligand Phbox-R exhibits free rotation along the phenyloxazoline axes. Upon coordination this rotation is restricted by an energy barrier of 26.0 kcal mol^{-1} for the case of $[Ru(trpy)(Phbox\text{-}iPr)(MeCN)]^{2+}$ thus preventing its potential interconversion. Furthermore due to steric effects the two atropisomers differ in energy by 5.7 kcal mol^{-1} and as a consequence only one of them is obtained in the synthesis. Subtle but important structural effects occur upon changing the monodentate ligands that are detected by NMR spectroscopy in solution and interpreted by using their calculated DFT structures.

Keywords: atropisomerism · chiral ligands · chirality · density functional calculations · ruthenium

Introduction

Ruthenium poly(pyridyl) complexes have been extensively studied over the years because they enjoy a combination of unique chemical, electrochemical, and photochemical properties[1] that have allowed the exploration of a wide variety of fields including photochemistry and photophysics,[2] bioinorganics,[3] and catalysis.[4] Recently, the dynamic behavior

[a] X. Sala, Dr. E. Plantalech, Dr. I. Romero, Dr. M. Rodríguez
Departament de Química, Universitat de Girona
Campus de Montilivi, 17071 Girona (Spain)
Fax: (+34) 972-418-150
E-mail: montse.rodriguez@udg.es

[b] Prof. Dr. A. Llobet
Departament de Química
Universitat Autònoma de Barcelona
Bellaterra, 08193 Barcelona (Spain)
Fax: (+34) 935-813-101
E-mail: antoni.llobet@uab.es

[c] A. Poater, Prof. Dr. M. Duran, Prof. Dr. M. Solà
Institut de Química Computacional
Universitat de Girona
Campus de Montilivi, 17071, Girona (Spain)
Fax: (+34) 972-418-356
E-mail: miquel.sola@udg.es

[d] Dr. S. Jansat, Dr. M. Gómez
Departament de Química Inorgànica
Universitat de Barcelona, Martí i Franquès
1–11, 08028 Barcelona (Spain)

[e] Dr. T. Parella
Servei de RMN, Universitat Autònoma de Barcelona Bellaterra, 08193 Barcelona (Spain)

[f] Dr. H. Stoeckli-Evans
Institute of Chemistry, University of Neuchatel
Av. Bellevaux 51, 2000, Neuchatel (Switzerland)

[g] Dr. J. Benet-Buchholz
Institut Català d'Investigació Química (ICIQ)
Avgda. Països Catalans, 16, 43007 Tarragona (Spain)

Supporting information (additional structural, spectroscopic, electrochemical, and computational data, as well as *x*,*y*,*z* coordinates of the computed complexes) for this article is available on the WWW under http://www.chemeurj.org/ or from the authors.

of ruthenium poly(pyridyl) complexes has played a key role in the understanding of artificial molecular-level machines[5] as well as in the elucidation of the factors affecting their binding to DNA.[6]

The generation, control, and induction of chirality is another very important field for the scientific and technological community.[7] Of special interest is atropisomerism, in which chirality is generated by the formation of two or more stable (non-interconverting) rotational isomers,[8] since it is potentially applicable to many different fields such as nanoscale information storage, chiral sensors, optoelectronics, as well as biomimetic and asymmetric catalysis among others.[9]

Considering this we have been working towards the design of atropisomeric Ru complexes where the chirality could be easily generated, controlled, and detected. Here, we present the synthesis, spectroscopic, and structural characterization of a new family of pure atropisomeric ruthenium complexes with general formula $[Ru(Y)(trpy)(Phbox\text{-}R)]^{n+}$ (Y = Cl, H_2O, py, MeCN, or 2-OH-py; trpy is 2,2′:6′,2″-terpyridine; Phbox-R is the chiral C_2–symmetric bidentate ligand 1,2-bis[4′-alkyl-4′,5′-dihydro-2′-oxazolyl]benzene; and 2-OH-py is 2-hydroxypyridine; Scheme 1), which signifies a step forward in our efforts to prepare new Ru complexes containing N-heterocyclic ligands.[10]

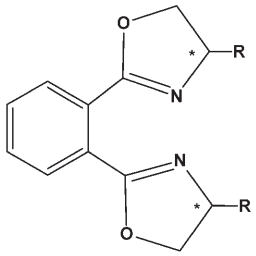

Phbox-**R**
(R = Et, (R_cR_c)-**a**; R = *i*Pr, (S_cS_c)-**b**)

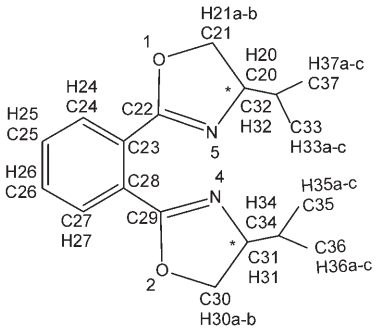

Phbox-*i*Pr, (S_cS_c)-**b**

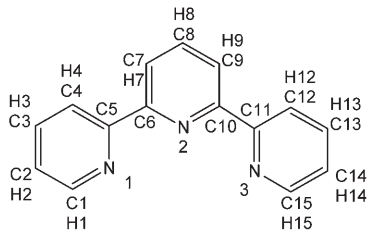

trpy

Scheme 1. Ligands employed in this work.

Results and Discussion

Synthesis and solid-state structure: The synthesis strategy followed for the preparation of the compounds described in the present paper is outlined in Scheme 2. The chiral ligands

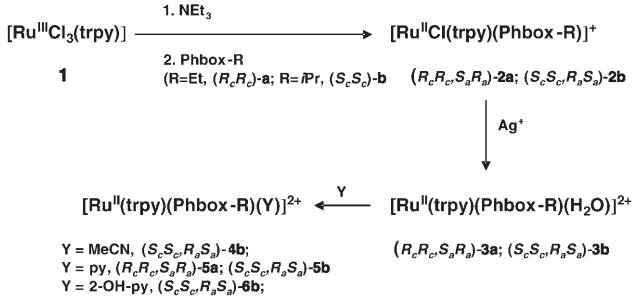

Scheme 2. Synthesis strategy for complexes **2**–**6** and their nomenclature.

have been prepared following the synthesis developed by Bolm et al.[11] In our ligand nomenclature, the capital letters refer to the absolute configuration of the two carbon stereocenters of the ligand and the "*c*" subscript indicates in each case that the stereochemistry is carbon-centered, to clearly establish a difference with the chirality originating from coordination of a ligand to the ruthenium center, denoted as "*a*" (see below for the nomenclature of complexes).

In the ligand syntheses, whereas the (S_cS_c)-**b** ligand is obtained in high optical purity, a mixture of two diastereoisomers, (R_cR_c)-**a**/(R_cS_c)-**a** (4:1), is obtained for the ligand **a** case. These two isomers can be separated by repeated recrystallization of the $[Ni(Phbox\text{-}Et)_2](ClO_4)_2$ complex followed by nickel-decomplexation.[12] On the other hand, the syntheses of complexes **2**–**6** have been carried out following slightly modified methods, previously described in the literature,[13] by using the didentate chiral bisoxazolinic ligands Phbox-R instead of 2,2′-bipyridine.

As denoted above, the nomenclature used for the complexes displays, through the first two letters, the absolute configuration of the carbon stereocenters in the ligand whereas the other two letters indicate the configuration of the rotation axes originating upon coordination of the oxazoline.

Figure 1 shows the chiral rotational axes in the two potential atropisomers, together with their nomenclature.

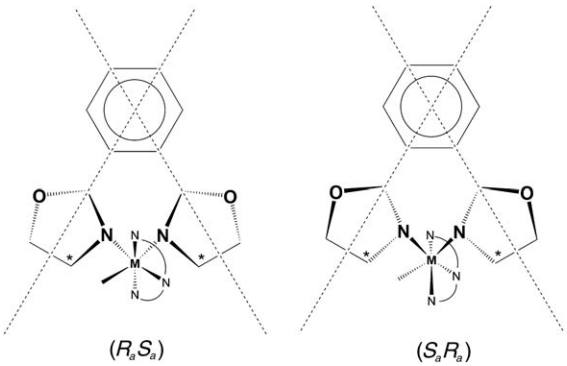

Figure 1. Drawing of the two atropisomeric forms generated by the bisoxazolinic ligand (Phbox-R) bonded to the Ru metal center. The chiral rotational axes are depicted with broken lines.

As displayed in Scheme 2, the Ru-aqua complexes (R_cR_c,S_aR_a)-**3a** or (S_cS_c,R_aS_a)-**3b**, that are obtained from the corresponding Ru-Cl complexes, (R_cR_c,S_aR_a)-**2a** and (S_cS_c,R_aS_a)-**2b** respectively, can be used as starting materials for the preparation of the Ru-MeCN ((S_cS_c,R_aS_a)-**4b**) and Ru-pyridino ((R_cR_c,S_aR_a)-**5a,** (S_cS_c,R_aS_a)-**5b** and (S_cS_c,R_aS_a)-**6b**) complexes. In the case of (R_cR_c,S_aR_a)-**5a** and (S_cS_c,R_aS_a)-**5b**, the reaction must be carried out at room temperature since higher temperatures induce the substitution of the oxazolinic ligand, besides the aqua ligand, yielding the $[Ru^{II}(trpy)(py)_3]^{2+}$ complex.[14] In the case of (S_cS_c,R_aS_a)-**6b**, that contains the 2-hydroxypyridine ligand, the reaction has to be carried out in the presence of molecular-sieves otherwise small amounts of water displace this ligand to generate the initial (S_cS_c,R_aS_a)-**3b** Ru-aqua complex due to the steric hindrance generated by the hydroxy group.

Crystallographic data for complexes (R_cR_c,S_aR_a)-**2a** and (S_cS_c,R_aS_a)-**4b** are presented in Table 1, whereas Figure 2 shows an ORTEP view of their cationic moieties. Further crystallographic data are presented in the Supporting Information.

Table 1. Crystal data for X-ray structures of (R_cR_c,S_aR_a)-**2a** and (S_cS_c,R_aS_a)-**4b**.

	(R_cR_c,S_aR_a)-**2a**	(S_cS_c,R_aS_a)-**4b**
empirical formula	$C_{31}H_{31}ClF_6N_5O_2PRu$	$C_{70}H_{76}B_4F_{16}N_{12}ORu_2$
formula weight	787.1	1650.81
crystal system	orthorhombic	triclinic
space group	$P2_12_12_1$	$P1$
a[Å]	10.4726(6)	8.8020(5)
b[Å]	13.0304(9)	11.0777(6)
c[Å]	23.0450(13)	19.1883(11)
α[°]	90	88.844(3)
β[°]	90	82.570(2)
γ[°]	90	79.829(2)
V[Å^3]	3144.8(3)	1826.10(18)
formula units/cell	1	1
ρ_{calcd}[g cm^{-3}]	1.663	1.501
μ[mm^{-1}]	0.055	0.507
absolute structure parameter	−0.03(3)	0.05(2)
R_1[a] ($I>2\sigma(I)$)	0.0337	0.0551
wR_2[b] (all data)	0.0563	0.1282

[a] $R_1=\Sigma||F_o|-|F_c||/\Sigma|F_o|$. [b] $wR_2=[\Sigma\{w(F_o^2-F_o^2)^2\}/\Sigma\{w(F_o^2)^2\}]^{1/2}$, where $w=1/[\sigma^2F_o^2+(m)^2+nP]$ and $P=(F_o^2+2F_c^2)/3$.

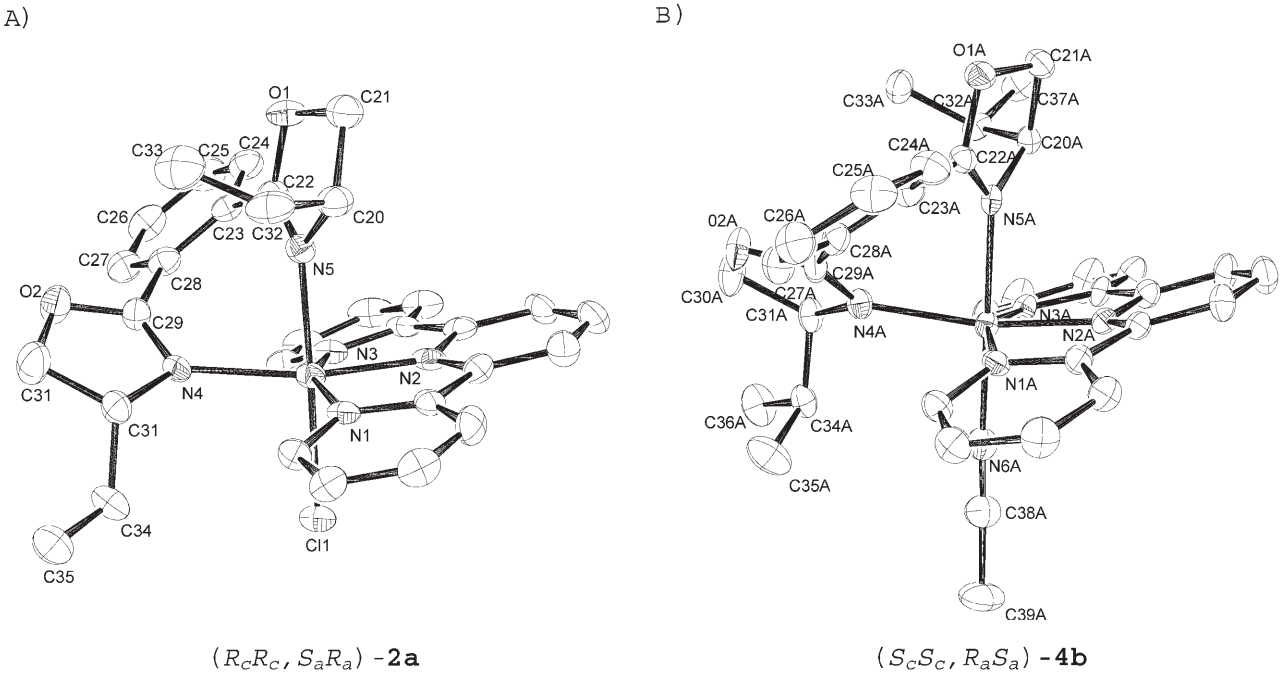

(R_cR_c,S_aR_a)-**2a** (S_cS_c,R_aS_a)-**4b**

Figure 2. ORTEP diagram (50% probability) for the cationic moieties of complexes (R_cR_c,S_aR_a)-**2a** (A) and (S_cS_c,R_aS_a)-**4b** (B).

In the Ru-Cl complex (R_cR_c,S_aR_a)-**2a**, the Ru metal atom presents a distorted octahedral coordination with the trpy ligand tricoordinated with its N atoms in a meridional fashion while the oxazolinic ligand coordinates also through its N atoms in a chelate manner. The remaining sixth coordination position is occupied by the chloro ligand. The bond lengths and angles involved in the first coordination sphere between the Ru^{II} metal center and the trpy, oxazoline, and Cl ligands are similar to related complexes previously described in the literature.[15] The bis(oxazoline) ligand forms a seven-membered chelate ring upon coordination to the Ru metal center with a bite angle of 82.4°[16] and with the two oxazolinyl rings being nearly perpendicular to one another (81.2°). Finally the dihedral angle between the best-adjusted planes defined by each oxazolinyl ring and the phenyl group are 40.9° and 55.5° for the oxazolinic groups containing N5 and N4 atoms, respectively. The phenyl group is situated over the N3 peripheral pyridyl group of the trpy ligand with a dihedral angle between the best-adjusted planes defined by these aromatic groups of 22.6°. The other atropisomer (R_cR_c,R_aS_a)-**2a**, can be potentially obtained through a partial rotation around the chiral axes depicted in Figure 1 (see below for a more detailed description of the different stereoisomers). This involves a simultaneous inverse rotation of two sigma C–C bonds (C29–C28 and C22–C23) that link the phenyl group with the oxazolinic moieties, driving the phenyl group of the (R_cR_c)-**a** ligand over the other N1 peripheral trpy pyridylic ring. It is interesting to note here that the steric demands of the (R_cR_c)-**a** oxazolinic moiety situated over the N3 trpy pyridyl group produces a significant dihedral angle between the N3 peripheral pyridyl group and the central N2 pyridyl group of 9.6°. In sharp contrast, the measured equivalent dihedral angle for the other pyridyl group containing N1, that is not directly affected by the steric demands of the (R_cR_c)-**a** ligand, is 4.4°. This value is comparable to other Ru-trpy complexes where no steric effects are exerted over the trpy ligand as is the case for the $[Ru^{III}Cl_3(trpy)]$ complex, that shows a medium dihedral angle between the peripheral and central pyridyl groups of 4.2°.[14]

All F atoms of the PF_6^- counter anions are interacting with the C–H bonds of the trpy and (R_cR_c)-**a** ligands of the $[Ru^{II}Cl(trpy)(Phbox\text{-}Et)]^+$ cation through extensive, moderate-to-weak hydrogen bonding, forming a three-dimensional network over the crystal. There are also relatively strong π–π stacking interactions[17] within neighboring cations through their peripheral pyridyl groups.

The crystal structure of complex (S_cS_c,R_aS_a)-**4b** presents two independent but very similar molecules; only the molecule labeled "A" will be discussed in the present paper. The structures are very similar to that of (R_cR_c,S_aR_a)-**2a** except for: a) the coordination of the monodentate ligand and b) the fact that the other atropisomer is obtained due to the opposite chiral configuration of the oxazolinic ligand.

Stereoisomeric analysis and DFT-calculated gas-phase structures: The C_2-symmetric free ligands, (R_cR_c)-**a** and (S_cS_c)-**b**, exhibit free rotation around the C–C bonds that link the aromatic ring with the oxazolinic moieties. Upon coordination to the metal center, the rotation is restricted leading to two limiting orientations as shown in Figure 1, thus generating two interdependent chiral axes that lead to atropisomerism. For the case of the (R_cR_c)-**a** ligand one could potentially obtain two diastereoisomers: the (R_cR_c,S_aR_a)- and the (R_cR_c,R_aS_a)-$[[Ru^{II}(Y)(trpy)(Phbox\text{-}Et)]^{n+}$ (Y = Cl, H_2O, or py). Experimental evidence, both in the solid state (X-ray diffraction, vide supra) and in solution (NMR spectroscopy, vide infra) indicates the existence of only the (R_cR_c,S_aR_a) isomer in all complexes containing the (R_cR_c)-**a** ligand and the other atropisomeric (S_cS_c,R_aS_a) complex for the case of the (S_cS_c)-**b** ligand. In both cases, the atropisomer obtained is the one that points the R groups of the oxazolinic rings away from the trpy plane, as expected from steric arguments. The fact that only one atropisomer is found in each case is in agreement with the presence of a large rotational barrier to interconvert the two atropisomers as can be further inferred from molecular models.

DFT calculations for a series of complexes containing the oxazolinic ligand (S_cS_c)-**b** were performed to deepen our understanding of the structure of these complexes and to obtain energy-barrier information about the atropisomeric interconversion.

Table 2 lists selected structural parameters obtained from X-ray data for (R_cR_c,S_aR_a)-**2a** and (S_cS_c,R_aS_a)-**4b**, together with the computed counterpart for (S_cS_c,R_aS_a)-**4b**. It also contains the computed (S_cS_c,S_aR_a)-**4b**, TS-**4b** (the transition state (TS) connecting the two isomers), (S_cS_c,R_aS_a)-**5b**, and two different conformers of (S_cS_c,R_aS_a)-**6b**, labeled "in" and "out" depending on the relative orientation of the hydroxy group versus the phenyl group of the oxazolinic ligand (towards N3 or N1 of the trpy ligand respectively, see Figure 4).

As shown in Table 2, the experimental and theoretical bond lengths and angles for (S_cS_c,R_aS_a)-**4b** differ by less than 0.07 Å and 3.0°, respectively. The standard deviation for the lengths is 0.043 Å and for the angles 0.25°.[18] These results validate the adequacy of the theoretical method employed for the geometry optimization of these particular systems.

Density functional theory (DFT) calculations for the two atropisomeric **4b** complexes yield a 5.7 kcal mol^{-1} energy difference in favor of the (S_cS_c,R_aS_a)-**4b** isomer in agreement with the experimental findings. The calculated structures (Figure 3) of the two isomers show that for the most stable isomer, the oxazolinic alkyl groups have a lower steric hindrance with respect to the trpy ligand. Figure 3 depicts the relative energies of the **4b** isomers including the TS that can be attained through the simultaneous inverse rotation of the chiral axes (see Figures 2 and 3). The high computational cost has prevented us from fully characterizing this stationary point as a TS by calculating the harmonic frequencies. However, we have checked that geometry optimization after a slight movement of the ring in both directions starting from the TS leads to the two initial atropisomers, one for

Table 2. Selected geometrical parameters for X-ray structures of (R_cR_c,S_aR_a)-**2a** and (S_cS_c,R_aS_a)-**4b** complexes, and for BPW91-optimized geometries of (S_cS_c,R_aS_a)-**4b**, (S_cS_c,S_aR_a)-**4b**, TS-**4b**, (S_cS_c,R_aS_a)-**5b**, *in*-(S_cS_c,R_aS_a)-**6b**, and *out*-(S_cS_c,R_aS_a)-**6b** complexes.

	(R_cR_c,S_aR_a)-**2a** (X-ray)	(S_cS_c,R_aS_a)-**4b**, A (X-ray)	(S_cS_c,R_aS_a)-**4b**	(S_cS_c,S_aR_a)-**4b**	TS-**4b**	(S_cS_c,R_aS_a)-**5b**	*in*-(S_cS_c,R_aS_a)-**6b**	*out*-(S_cS_c,R_aS_a)-**6b**
Ru–N1	2.122(3)	2.057(4)	2.125	2.126	2.122	2.114	2.115	2.094
Ru–N2	1.947(4)	1.954(4)	1.991	1.986	1.981	1.985	1.978	1.977
Ru–N3	2.087(4)	2.100(4)	2.148	2.124	2.104	2.166	2.146	2.151
Ru–N4	2.180(4)	2.146(4)	2.191	2.184	2.230	2.218	2.215	2.208
Ru–N5	2.086(4)	2.083(4)	2.127	2.149	2.149	2.141	2.157	2.147
Ru–Z[a]	2.415(1)	2.018(4)	2.040	2.041	2.050	2.203	2.222	2.231
N3-Ru-N2	79.52(15)	78.64(14)	78.06	78.57	79.39	77.90	78.04	78.01
N3-Ru-N1	156.27(14)	156.13(14)	154.94	156.78	158.65	156.41	157.13	157.30
N2-Ru-N1	78.08(14)	79.62(14)	78.28	78.31	79.27	78.75	79.09	79.30
N2-Ru-N4	169.12(15)	167.30(14)	169.89	178.45	176.71	170.14	172.09	171.60
N4-Ru-N5	82.37(14)	83.25(14)	82.99	91.02	93.68	82.76	84.68	84.82
N3-Ru-Z[a]	87.22(9)	88.15(15)	88.63	88.51	90.55	88.65	91.38	86.29
N2-Ru-Z[a]	94.82(12)	95.42(16)	94.30	88.41	80.28	93.13	89.95	92.36
N1-Ru-Z[a]	86.95(11)	84.21(15)	85.01	88.72	85.30	89.31	88.52	94.51
N4-Ru-Z[a]	96.01(10)	96.62(16)	99.57	90.12	96.50	96.43	97.78	97.78
N5-Ru-Z[a]	177.89(12)	179.40(17)	178.35	178.05	168.99	178.86	177.55	175.39

[a] For (R_cR_c,S_aR_a)-**2a**, Z is Cl; for the other complexes, Z is N6.

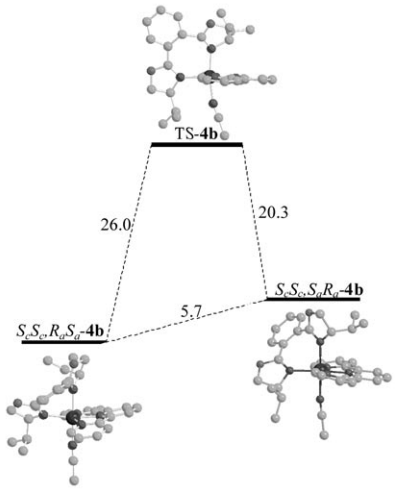

Figure 3. Relative energy diagram for the two possible atropisomers, (S_cS_c,R_aS_a)-**4b** and (S_cS_c,S_aR_a)-**4b**, and the transition state connecting them, TS-**4b**. Energies are given in kcal mol^{-1}.

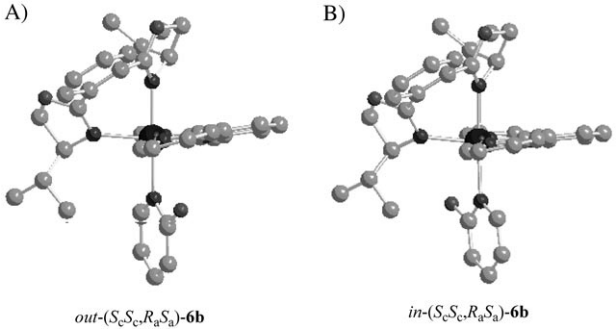

Figure 4. BPW91-optimized geometries of the cationic moieties of two (S_cR_c,S_aS_a)-**6b** conformers with relatively similar energy but with different orientations of the 2-hydroxypyridine group; A) *out*-(S_cS_c,R_aS_a)-**6b** and B) *in*-(S_cS_c,R_aS_a)-**6b**.

each direction. The 26.0 kcal mol^{-1} energy barrier to interconvert the two atropisomers further agrees with the experimental finding that no interconversion is taking place in solution from one isomer to the other at room temperature. The relatively large energy barrier is due to the highly tensioned nearly planar seven-membered chelating ring that the oxazoline ligand adopts in the TS as depicted in Figure 3.

Drawings of the calculated gas-phase structures for the 2-hydroxypyridine complexes out-(S_cS_c,R_aS_a)-**6b** and in-(S_cS_c,R_aS_a)-**6b** are displayed in Figure 4 A and B, respectively (Cartesian coordinates of these complexes are given in the Supporting Information). The most prominent difference of the Ru-(2-OH-py) (S_cS_c,R_aS_a)-**6b** and the Ru-MeCN (S_cS_c,R_aS_a)-**4b** structures is the fact that in the Ru-(2-OH-py) complexes the trpy pyridylic rings are more coplanar due to the steric hindrance generated by the perpendicular pyridine ligand. The energy difference between the *in*-(S_cS_c,R_aS_a)-**6b** and *out*-(S_cS_c,R_aS_a)-**6b** isomers is only 0.6 kcal mol^{-1} in the gas phase. We have found that this energy difference remains almost unaltered (0.5 kcal mol^{-1}) when the solvent effect is considered in our calculations and thus it can be inferred that in solution they will easily interconvert.

Solution structure and NMR spectroscopy: NMR data for complexes **2–6** are listed in the Experimental Section and the most significant chemical shifts and NOE contacts are reported in Table 3. All the labels used with the NMR data are keyed with regard to the labels used in the crystal structure of (S_cS_c,R_aS_a)-**4b**. The numbering scheme is given in Scheme 1.

The absence of symmetry in the ruthenium complexes described in the present work renders all their hydrogen atoms to be magnetically different. It has been possible to assign

Table 3. Selected NMR data for (S_cS_c,R_aS_a)-**2b**, (S_cS_c,R_aS_a)-**3b**, (S_cS_c,R_aS_a)-**4b**, (S_cS_c,R_aS_a)-**5b**, and (S_cS_c,R_aS_a)-**6b** complexes.

		(S_cS_c,R_aS_a)-**2b**	(S_cS_c,R_aS_a)-**3b**	(S_cS_c,R_aS_a)-**4b**	(S_cS_c,R_aS_a)-**5b**	(S_cS_c,R_aS_a)-**6b**
trpy[a]	H1	7.95	7.97	7.92	8.10	8.97
	H15	9.41 (H31, H34, H32)	9.46 (H31, H34, H32)	9.35 (H31, H34, H32, H36)	9.32 (H31, H34, H36)	9.00 (H31)
Ph-Ox	H24	7.26	7.25	7.31	7.33	6.27
	H25	7.57	7.58	7.60	7.65	7.22
	H26	7.90	7.95	7.92	7.98	5.83
	H27	8.13	8.20	8.21	8.20	6.12
CH-Ox5	H20	2.97	2.91	3.15	3.14	3.58
CH_2-Ox5	H21a	4.31	4.29	4.43	4.39	3.91
CH_2-Ox5	H21b	3.82	3.84	3.99	3.92	4.35
CH-*i*Pr5	H32	1.11	1.06	1.18	1.03	1.50
Me-*i*Pr5	H33a–c	0.28	0.25	0.28	0.28	0.67
Me-*i*Pr5	H37a–c	0.53	0.57	0.58	0.55	0.70
CH-Ox4	H31	5.56	5.67	5.64	5.4	4.58
CH_2-Ox4	H30a	5.16	5.20	5.14	5.20	4.54
CH_2-Ox4	H30b	5.00	5.11	5.12	5.07	4.13
CH-*i*Pr4	H34	3.72	2.88	3.04	1.51	3.54
Me-*i*Pr4	H36a–c	1.13	1.18	1.30	1.02	0.85
Me-*i*Pr4	H35a–c	1.18	1.21	1.30	1.20	1.17

[a] The most significant NOE contacts are indicated in brackets.

all the resonances from the fine structure of their 1D and 2D NMR spectra. It is important to emphasize the importance of the chirality of the C_2-symmetric Phbox-R ligands in order to detect and characterize the atropisomeric complexes through NMR spectroscopy. With R = H, the corresponding achiral oxazolinic ligand, the two enantiomeric atropisomers would have been magnetically indistinguishable.

The ^{1}H NMR spectrum of the Ru-Cl complex, (S_cS_c,R_aS_a)-**2b**, demonstrates that in solution the structure is very similar to the one obtained in the solid state, as is expected for this type of Ru d^6 complex. The most interesting feature of the structure is the fact that one of the oxazoline groups of the Phbox-*i*Pr ligand, (S_cS_c)-**b**, containing the N5 atom and referred to as Ox5 (see also Table 3 for the general terms used to described the different groups of the ligands), is situated very close to the N3 peripheral pyridylic group and thus suffers a strong anisotropic current-field effect producing a significant upfield displacement of all their resonances (compare Ox5 with Ox4 in Table 3). The most affected resonance corresponds to the CH group of the *i*Pr substituent, termed CH-*i*Pr5, which is shifted by approximately 2.6 ppm relative to CH-*i*Pr4. Another important outcome of the NMR study of complex (S_cS_c,R_aS_a)-**2b** is the interligand NOE contacts observed between the H15 atom from the N3 peripheral pyridylic ring of the trpy ligand and the H31 and H34 atoms from CH-Ox4 and CH-*i*Pr4 respectively (see Table 3), which also indicate the relative position of the Ox4 group with regard to the trpy ligand.

Table 3 shows that nearly all the resonances and NOE contacts of complexes (S_cS_c,R_aS_a)-(**2b**–**5b**) are very similar, and thus it can be concluded that they must exhibit the same type of structure in solution. However some differences are found; for instance it is worth noting that for the Ru-pyridine complex (S_cS_c,R_aS_a)-**5b** the CH-*i*Pr4 resonance is significantly shifted upfield with regard to the (S_cS_c,R_aS_a)-(**2b**–**4b**) complexes due to the current field of the pyridine ligand. The fact that the resonances for the Me-*i*Pr4 are not shifted as expected suggests that the *i*Pr4 group is not freely rotating but, on the contrary, it remains relatively frozen due to the steric congestion due to the presence of the pyridine ligand. This is further supported by the fact that the pyridine ligand is rapidly rotating along the Ru–N bond as deduced from the magnetic equivalence of their *ortho*- and *meta*-H atoms, under the NMR experimental conditions, given the asymmetry of the rest of the complex. Those *ortho*- and *meta*-H atoms present NOE contacts with both H1 and H15 atoms from the trpy ligand, further corroborating the previous statement.

Table 3 also shows that the solution structure of the 2-OH-pyridine Ru complex, (S_cS_c,R_aS_a)-**6b**, is notably different from the rest of the complexes. As mentioned in the previous section, DFT calculations show the existence of two conformers with relatively close energies, suggesting again that in solution, the 2-OH-pyridine ligand is also rotating through the Ru–N bond. An interesting feature of the *in*-(S_cS_c,R_aS_a)-**6b** and *out*-(S_cS_c,R_aS_a)-**6b** structures, and especially for the "*in*" case, is that the angle between the best-adjusted planes that describe the two oxazolinic rings is significantly increased with regard to the other complexes described in this work including the Ru-py complex (S_cS_c,R_aS_a)-**5b** (73.4° for (S_cS_c,R_aS_a)-**5b**, 89.6° for *in*-(S_cS_c,R_aS_a)-**6b** and 78.9° for *out*-(S_cS_c,R_aS_a)-**5b**; see the Supporting Information for other angles between different rings). This angle increase, with regard to the Ru-py case, is due to the large steric hindrance produced by the OH group of the 2-OH-py ligand against the *i*Pr4 group that in turn generates a slight rotation of the chiral axes to accommodate itself. This produces a synchronized inverse-rotation of the oxazolinic rings taking the *i*Pr4 group further from the Ru center and the trpy ligand, and moving the phenyl oxazolinic group closer to the peripheral N1 pyridylic trpy group. The former effect is also corroborated by the non-existence of the NOE contacts between H15–H34 in (S_cS_c,R_aS_a)-**6b** (see Figure 5) in sharp contrast with the fact that it is observed for all the other complexes described in this work. The latter is also corroborated by the chemical

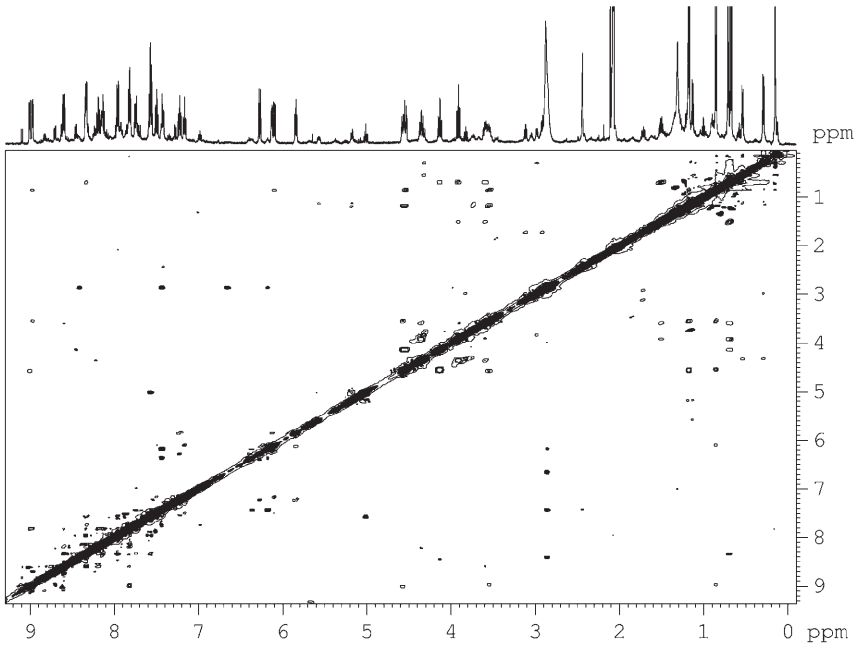

Figure 5. NOESY NMR spectrum of (S_cS_c,R_aS_a)-**6b**.

shifts of the H26 and H27 atoms (Table 3) that no longer tend to increase but decrease by roughly 2 ppm with regard to their related pyridine complex, suggesting an anisotropic influence of the trpy aromatic field towards these two hydrogen atoms.

In conclusion, the chirality of the 1,2-bis(oxazolinyl)benzene ligand Phbox-R, either (R_cR_c) or (S_cS_c), allows us to prepare and isolate pure atropisomeric complexes due to the highly restricted rotation along the oxazolinic–phenyl axes induced upon coordination to a Ru metal center. A family of atropisomeric complexes has thus been isolated and fully characterized in the solid state by X-ray diffraction analysis, in solution by mainly NMR spectroscopy, and in the gas phase by means of DFT calculations. This thorough structural characterization yields a very complete and coherent discription of these types of complex with a surprisingly detailed description of mononuclear-ligand effects towards both bis(oxazolinic)- and trpy-coordinated ligands.

Experimental Section

Materials: All reagents used in the present work were obtained from Aldrich Chemical Co. and were used without further purification. Reagent-grade organic solvents were obtained from SDS and high purity deionized water was obtained by passing distilled water through a nanopure Milli-Q water purification system. $RuCl_3{\cdot}2H_2O$, was supplied by Johnson and Matthey Ltd. and was used as received.

Instrumentation and measurements: IR spectra were recorded on a Mattson Satellite FTIR with KBr pellets or by using an MKII Golden Gate Single-Refraction ATR System. UV/Vis spectroscopy was performed in a Cary 50 Scan (Varian) UV/Vis spectrophotometer with 1 cm quartz cells. Measurements of pH were made using a Micro-pH-2000 from Crison. Cyclic voltammetry (CV) experiments were performed in PAR 263 A EG&G or IJ-Cambria IH-660 potentiostats, by using a three-electrode cell. Glassy carbon disk electrodes (3 mm diameter) from BAS were used as the working electrode, a platinum-wire electrode was used as the auxiliary, and SSCE as the reference electrode. Cyclic voltammograms were recorded at 100 $mV\,s^{-1}$ scan rate under nitrogen atmosphere. The complexes were dissolved in previously degassed solvents containing the necessary amount of supporting electrolyte to yield a solution of 0.1 M ionic strength. $(n\mathrm{Bu_4N})(PF_6)$ was used as the supporting electrolyte when using acetonitrile and dichloromethane solvents. All $E_{1/2}$ values reported in this work were estimated from CV measurements as the average of the oxidative and reductive peak potentials $(E_{p,a}+E_{p,c})/2$. Unless explicitly mentioned the concentrations of the complexes were approximately 1 mM.

The ^{1}H NMR spectroscopy was performed on a Bruker DPX 200 MHz, a Bruker DPX 250 MHz, or a Varian VRX 500 MHz spectrometer. Samples were run in $[D_6]$acetone or deuterium oxide with internal references (residual protons and/or tetramethylsilane, or DSS respectively). Elemental analyses were performed using a CHNSO Elemental Analyser EA-1108 from Fisons Instruments. The FAB mass spectroscopy experiments were performed on a VG-QUATTRO spectrometer from Fisons Instruments.

X-ray structure determination: Suitable crystals of (R_cR_c,S_aR_a)-**2a** were grown by slow diffusion of ether into a solution containing methanol as dark red blocks and suitable crystals of (S_cS_c,R_aS_a)-**4b** were grown by slow diffusion of ether into a acetonitrile solution as dark-red needles or plates.

Data collection: Intensity data of complex (R_cR_c,S_aR_a)-**2a** were collected at 193 K on a Stoe Image-Plate Diffraction System equipped with a φ circle, using $Mo_{K\alpha}$ graphite-monochromated radiation ($\lambda = 0.71073$ Å) with φ range 0–150°, increment 1°, 2θ range 4.0–52.0°, D_{min}–D_{max} 12.45–0.81 Å. Measurements of complex (S_cS_c,R_aS_a)-**4b** were made on a Siemens P4 diffractometer equipped with a SMART-CCD-1000 area detector, a MACScience Co. rotating anode with $Mo_{K\alpha}$ radiation, a graphite monochromator, and a Siemens LT2 low-temperature device ($T = -120$ °C). Full-sphere data collection with ω and ϕ scans. Programs used: data collection, Smart Version 5.060 (Bruker AXS, 1999); data reduction, Saint+ Version 6.02 (Bruker AXS, 1999); absorption correction, SADABS (Bruker AXS, 1999).

Structure solution and refinement: The structures were solved by direct methods using the program SHELXS-97.[19a] The refinement and all further calculations were carried out using SHELXL-97.[19b] Hydrogen atoms were included in calculated positions and treated as riding atoms by using SHELXL-97 default parameters (AFIX 137 for the methyl H atoms). The non-hydrogen atoms were refined anisotropically by using weighted full-matrix least-squares on F^2. The absolute structure parameters[20] were −0.03(3) for (R_cR_c,S_aR_a)-**2a** and 0.05(2) for (S_cS_c,R_aS_a)-**4b** indicating that the coordinates corresponded to the correct absolute structure of the molecule in the crystals under study. The molecular structures and crystallographic numbering schemes are illustrated in the ORTEP drawings in Figures 2 A ((R_cR_c,S_aR_a)-**2a**) and B ((S_cS_c,R_aS_a)-**4b**, molecule A) (thermal ellipsoids were drawn at 50% probability). The asymmetric unit in the crystal of (S_cS_c,R_aS_a)-**4b** contains two independent molecules of the complex. Due to the similarities only molecule A will be considered for discussion. Its crystallographic parameters are shown in Table 1,

and some selected bond lengths and angles can be found in the Supporting Information. CCDC-263477 and CCDC-263478 contain the supplementary crystallographic data for this paper. These data can be obtained free of charge from the Cambridge Crystallographic Data Centre via www.ccdc.cam.ac.uk/data_request/cif.

Computational details: The reported DFT calculations were carried out by using the Amsterdam density functional (ADF)[21] program system developed by Baerends and co-workers. The numerical integration scheme employed was that of te Velde and Baerends.[22] An uncontracted triple-ζ basis set[23] was used for describing the 4s, 4p, 4d, 5s, and 5p orbitals of ruthenium. For carbon (2s,2p), nitrogen (2s,2p), oxygen (2s,2p), and hydrogen (1s), double-ζ basis sets were employed. Both basis sets were augmented by an extra polarization function.[23] Electrons in lower shells were treated within the frozen-core approximation.[21c] A set of auxiliary s, p, d, f, and g functions,[24] centered in all nuclei, was introduced in order to fit the molecular density and Coulomb potential accurately in each SCF cycle. Both geometry optimizations and energy evaluations have been fully carried out within a DFT generalized-gradient-approximation (GGA) functional that includes the GGA exchange and correlation corrections of Becke,[25] and Perdew and Wang,[26] (BPW91) respectively.

The solvent effect was included in the calculation of the relative energy of complexes *in*-(S_cS_c,R_aS_a)-**6b** and *out*-(S_cS_c,R_aS_a)-**6b** through single-point-energy calculations by the conductor-like screening model (COSMO) of Klamt and Schüürmann,[27] implemented into the ADF program by Pye and Ziegler.[28] The radius chosen for the solvent (3.02 Å) was obtained with the GAUSSIAN98 package[29] from the calculated molecular volume of acetone ($\varepsilon = 21.01$),[30] that was the solvent used in the NMR characterization. The radii used for C, O, N, H, and Ru were 1.53, 1.36, 1.48, 1.08, and 2.30 Å, respectively.[31] Finally the dihedral angle between the best-adjusted planes defined by two groups of atoms was measured by the Spartan′02 program.[32]

Preparation: The Phbox-R (R = Et, (R_cR_c)-**a**; *i*Pr, (S_cS_c)-**b**; see Scheme 1) ligands[11] and the [$Ru^{III}Cl_3$(trpy)] complex **1**[33] were prepared according to literature procedures. All synthesis manipulations were routinely performed under nitrogen atmosphere using Schlenck tubes and vacuum-line techniques. Electrochemical experiments were performed under either N_2 or Ar atmosphere with degassed solvents.

The subsequent nomenclature used regarding the absolute configuration of the complexes described is as follows: the first two letters refer to the absolute configuration of the oxazolinic ligand whereas the other two letters refer to the absolute configuration of the chiral rotational axes (see Figure 1).

(R_cR_c,S_aR_a)-[Ru^{II}Cl(trpy)(Phbox-Et)](BF_4)·H_2O, (R_cR_c,S_aR_a)-2a·H_2O: A sample of compound **1** (200 mg, 0.454 mmol) was added to a 100 mL round-bottomed flask containing a solution of LiCl (27 mg, 0.645 mmol) in EtOH/H_2O (3:1 v/v) (40 mL), with magnetic stirring. Then, NEt_3 (110 mL) was added and the reaction mixture was stirred at room temperature for 30 min at which point Phbox-Et (123 mg, 0.454 mmol) was added and the mixture was heated under reflux for 3.5 h. The hot solution was filtered through a frit and the solution was reduced to dryness in a rotary evaporator under reduced pressure after the addition of an aqueous saturated solution of $NaBF_4$ (1.5 mL). The solid obtained was then dissolved in CH_2Cl_2 and washed several times with water. The organic phase was then dried over $MgSO_4$ and the solution was again reduced to dryness. The solid obtained in this manner was then recrystallized from a hot mixture of MeOH/diethyl ether (1:1 v/v). A black dust was obtained that was captured on a frit, was washed with a small amount of cold MeOH, and was dried under vacuum. Yield: 58.4% (198 mg, 0.264 mmol); ^{1}H NMR (200 MHz, [D_6]acetone, 25°C): $\delta = 0.35$ (t, $^3J_{33a,32} = 7.6$ Hz, 3H; H33a–c), 0.80 (m, 2H; H32a–b), 1.11 (t, $^3J_{35,34} = 7.4$ Hz, 3H; H35a–c), 2.23 (m, 1H; H34b), 2.73 (m, 1H; H34a), 2.91 (m, 1H; H20), 3.91 (pt, $J = 8.8$ Hz, 1H; H21b), 4.18 (dd, $^3J_{21a,20} = 2.2$, $^2J_{21a,21b} = 9.2$ Hz, 1H; H21a), 5.11 (m, 2H; H30a–b), 5.35 (m, 1H; H31), 7.01 (dt, $^3J_{14,15} = {}^3J_{14,13} = 7.2$ Hz, $^3J_{14,12} = 1.2$ Hz, 1H; H14), 7.40 (dd, $^3J_{24,25} = 8.0$ Hz, $^3J_{24,26} = 1.2$ Hz, 1H; H24), 7.65 (dt, $^3J_{25,24} = {}^3J_{25,26} = 8.0$ Hz, $^3J_{25,27} = 1.4$ Hz, 1H; H25), 7.75–7.86 (m, 2H; H2, H13), 7.90–8.05 (m, 3H; H3, H8, H26), 8.24 (dd, $^3J_{27,26} = {}^3J_{12,13} = 8.0$ Hz, $^3J_{12,14} = 1.2$ Hz, $^3J_{27,25} = 1.4$ Hz, 2H; H12, H27), 8.39 (d, $^3J_{15,14} = 7.2$ Hz, 1H; H15), 8.48 (d, $^3J_{9,8} = 7.8$ Hz, 1H; H9), 8.64 (d, $^3J_{7,8} = 8.0$ Hz, 1H; H7), 8.72 (d, $^3J_{4,3} = 8.2$ Hz, 1H; H4), 9.35 ppm (d, $^3J_{1,2} = 6.8$ Hz, 1H; H1); UV/Vis (CH_2Cl_2): $\lambda_{max} = 282$ ($\varepsilon = 20360$), 324 (26359), 370 (5617) 524 (5534) and 570 nm^{-1} (5202 dm^{3}mol^{-1} cm^{-1}); $E_{1/2}$ (MeCN): 0.700 V; elemental analysis calcd (%) for $C_{31}H_{33}BClF_4N_5O_3Ru$: C 49.5, H 4.1, N 9.2; found: C 49.8, H 4.4, N 9.4.

(S_cS_c,R_aS_a)-[Ru^{II}Cl(trpy)(Phbox-*i*Pr)](PF_6)·2.5H_2O, (S_cS_c,R_aS_a)-2b·2.5H_2O: This compound was prepared in the same manner as that above except that the equivalent amount of Phbox-*i*Pr was used instead of Phbox-Et and a saturated solution of KPF_6 was used instead of $NaBF_4$. Yield: 75.0% (292 mg, 0.304 mmol); ^{1}H NMR (500 MHz, [D_6]acetone, 25°C): $\delta = 0.28$ (d, $^3J_{33ac,32} = 7.2$ Hz, 3H; H33a–c), 0.53 (d, $^3J_{37ac,32} = 6.8$ Hz, 3H; H37a–c), 1.11 (m, 1H; H32)), 1.13 (d, $^3J_{36ac,34} = 7.4$ Hz, 3H; H36a–c), 1.18 (d, $^3J_{35ac,34} = 6.7$, 3H; H35a–c), 2.97 (m, 1H; H20), 3.72 (m, 1H; H34), 3.82 (dd, $^3J_{21b,20} = 8.7$ Hz, $^2J_{21b,21a} = 9.3$ Hz, 1H; H21b), 4.31 (dd, $^3J_{21a,20} = 2.5$ Hz, $^2J_{21a,21b} = 9.3$ Hz, 1H; H21a), 5.00 (dd, $^3J_{30b,31} = 4.9$ Hz, $^2J_{30b,30a} = 9.3$ Hz, 1H; H30b), 5.16 (dd, $^3J_{30a,31} = 4.9$, $^3J_{30a,30b} = 9.3$ Hz, 1H; H30a), 5.56 (m, 1H; H31), 6.96 (ddd, $^4J_{2,4} = 1.2$ Hz, $^3J_{2,1} = 7.2$ Hz, $^3J_{2,3} = 7.7$ Hz, 1H; H2), 7.26 (dd, $^4J_{24,26} = 1.2$ Hz, $^3J_{24,25} = 7.8$ Hz, 1H; H24), 7.57 (td, $^4J_{25,27} = 1.2$ Hz, $^3J_{25,24} = {}^3J_{25,26} = 7.8$ Hz, 1H; H25), 7.71 (td, $^4J_{3,1} = 1.3$, $^3J_{3,2} = {}^3J_{3,4} = 7.7$ Hz, 1H; H3), 7.84 (ddd, $^4J_{14,12} = 1.2$ Hz, $^3J_{14,15} = 5.8$ Hz, $^3J_{14,13} = 7.2$ Hz, 1H; H14), 7.90 (td, $^4J_{26,24} = 1.2$ Hz, $^3J_{26,25} = {}^3J_{26,27} = 7.8$ Hz, 1H; H26), 7.93 (t, $^3J_{8,7} = {}^3J_{8,9} = 7.7$ Hz, 1H; H8), 7.95 (d, $^3J_{1,2} = 7.2$ Hz, 1H; H1), 8.13 (dd, $^4J_{27,25} = 0.9$ Hz, $^3J_{27,26} = 7.8$ Hz, 1H; H27), 8.21 (td, $^4J_{13,15} = 1.4$ Hz, $^3J_{13,14} = {}^3J_{13,12} = 7.2$ Hz, 1H; H13), 8.30 (d, $^3J_{4,3} = 7.7$ Hz 1H; H4), 8.44 (d, $^3J_{7,8} = 7.7$ Hz, 1H; H7), 8.60 (d, $^3J_{9,8} = 7.7$ Hz, 1H; H9), 8.69 (d, $^3J_{12,13} = 7.2$ Hz, 1H; H12), 9.41 ppm (d, $^3J_{15,14} = 5.8$ Hz, 1H; H15); UV/Vis (CH_2Cl_2): $\lambda_{max} = 284$ ($\varepsilon = 23139$), 322 (29822), 368 (6468), 530 (5342), 562 nm^{-1} (5585 dm^{3}mol^{-1} cm^{-1}); $E_{1/2}$ (CH_3CN): 0.71 V versus SSCE; elemental analysis calcd (%) for $C_{33}H_{35}N_5O_2RuClPF_6$·2.5$H_2O$: C 46.08, N 8.14, H 4.69; found: C 46.25, N 7.96, H 4.73.

(R_cR_c,S_aR_a)/(S_cS_c,R_aS_a)-[Ru^{II}(trpy)(Phbox-R)(H_2O)](BF_4)$_2$, (R_cR_c,S_aR_a)-3a/(S_cS_c,R_aS_a)-3b: A sample of $AgBF_4$ (64 mg, 0.329 mmol) was added to a mixture of acetone/H_2O (1:1 v/v, 30 mL) containing 2a·H_2O or 2b·2.5H_2O (0.200 mmol, 150 and 172 mg respectively) and was heated at reflux for 2 h. AgCl was filtered off through a frit containing celite and the volume was reduced in a rotary evaporator under reduced pressure until the solution began to appear turbid. Then it was cooled in an ice bath and the solid obtained was filtered on a frit, washed with a small amount of chilled water, and dried under vacuum. For (R_cR_c,S_aR_a)-**3a**, Yield: 57.6% (92 mg, 0.117 mmol); ^{1}H NMR (200 MHz, [D_6]acetone, 25°C): $\delta = 0.32$ (t, $^3J_{33,32} = 7.5$ Hz, 3H; H33a–c), 0.82 (m, 2H; H32a–b), 1.16 (t, $^3J_{35,34} = 7.5$ Hz, 2H; H35a–c), 2.22 (m, 2H; H34a–b), 2.87 (m, 2H; H20, H31), 3.94 (m, 2H; H21a–b), 4.20 (m, 2H; H30a–b), 4.62 (s, 2H; H_2O), 7.90–9.7 ppm (m, 15H; H1–H9, H12–H15, H24–H27); UV/ Vis (phosphate buffer pH 6): $\lambda_{max} = 280$ ($\varepsilon = 21538$), 316 (25538), 470 (sh), 518 nm^{-1} (4745 dm^{3}mol^{-1} cm^{-1}); UV/Vis (CH_2Cl_2): $\lambda_{max} = 282$ ($\varepsilon = 20215$), 318 (28681), 475 (es), 518 nm^{-1} (4935 dm^{3}mol^{-1} cm^{-1}); MS (70 eV, EI): *m*/*z* (%): 626.4 (76), 606.4 (48), 508.6 (17), 369.3 (35), 351.1 (74), 334.6 (100); $E_{1/2}$ (CH_2Cl_2): 0.98 V versus SSCE. For (S_cS_c,R_aS_a)-**3b**, Yield: 68% (74 mg, 0.089 mmol); ^{1}H NMR (500 MHz, [D_6]acetone, 25°C): $\delta = 0.25$ (d, $^3J_{33ac,32} = 7.0$ Hz, 3H; H33a–c), 0.57 (d, $^3J_{37ac,32} = 7.0$ Hz, 3H; H37a–c), 1.06 (m, 1H; H32), 1.18 (d, $^3J_{36ac,34} = 7.2$ Hz, 3H; H36a–c), 1.21 (d, $^3J_{35ac,34} = 11.1$ Hz, 3H; H35a–c), 2.88–2.91 (m, 2H; H34, H20), 3.84 (dd, $^3J_{21b,20} = 8.4$, $^2J_{21b,21a} = 9.3$ Hz, 1H; H21b), 4.29 (dd, $^3J_{21a,20} = 2.3$, $^2J_{21a,20} = 9.5$ Hz, 1H; H21a), 5.11 (dd, $^3J_{30b,31} = 5.8$, $^2J_{30b,30a} = 9.5$ Hz, 1H; H30b), 5.20 (dd, $^3J_{30a,31} = 5.7$, $^2J_{30a,30b} = 9.3$ Hz, 1H; H30a), 5.67 (dddd, $^3J_{31,30a} = 5.7$ Hz, $^3J_{31,30b} = 5.8$ Hz, $^3J_{31,34} = 6.7$ Hz, 1H; H31), 7.05 (ddd, $^4J_{2,4} = 1.2$ Hz, $^3J_{2,1} = 5.1$ Hz, $^3J_{2,3} = 7.9$ Hz, 1H; H2), 7.25 (dd, $^4J_{24,26} = 0.9$ Hz, $^3J_{24,25} = 7.9$ Hz, 3H; H24), 7.58 (td, $^4J_{25,27} = 1.2$ Hz, $^3J_{25,24} = {}^3J_{25,26} = 7.9$ Hz, 3H; H25), 7.83 (td, $J = {}^4J_{3,1} = 1.2$ Hz, $^3J_{3,2} = {}^3J_{3,4} = 7.9$ Hz, 1H; H3), 7.95–7.97 (m, 3H; H26, H14, H1), 8.10 (t, $^3J_{8,9} = {}^3J_{8,7} = 8.0$ Hz, 1H; H8), 8.20 (dd, $^4J_{27,25} = 1.2$ Hz, $^3J_{27,26} = 7.2$ Hz, 1H; H27), 8.33 (td, $^4J_{13,15} = 1.2$ Hz, $^3J_{13,14} = {}^3J_{13,12} = 7.8$ Hz, 1H; H13), 8.40 (d, $^3J_{4,3} = 7.9$ Hz, 1H; H4), 8.55 (d, $^3J_{7,8} = 8.0$ Hz, 1H; H7), 8.71 (d, $^3J_{9,8} = 8.0$ Hz, H9), 8.71 (d, $^3J_{12,13} = 7.8$ Hz, H12), 9.46 ppm (d, $^3J_{15,14} = 5.1$ Hz, H15); UV/Vis (phosphate buffer pH 6): $\lambda_{max} = 278$ ($\varepsilon = 17983$), 316 (22759), 484 (3672), 518 nm^{-1} (3724 dm^{3}mol^{-1} cm^{-1}); UV/Vis (CH_2Cl_2): $\lambda_{max} = 278$ ($\varepsilon = 28320$), 318

(29792), 486 (4989), 520 nm^{-1} (4950 $dm^3 mol^{-1} cm^{-1}$); $E_{1/2}$ (CH_2Cl_2): 0.98 V versus SSCE; elemental analysis calcd (%) for $C_{33}H_{37}N_5O_3RuB_2F_8$: C 47.97, N 8.48, H 4.48; found: C 48.06, N 8.39, H 4.77.

(S_cS_c,R_aS_a)-[Ru^{II}(trpy)(Phbox-*i*Pr)(MeCN)](PF$_6$)$_2$, (S_cS_c,R_aS_a)-4b: A sample of the aquacomplex (S_cS_c,R_aS_a)-**3b** (100 mg, 0.152 mmol) was dissolved in acetonitrile (25 mL) and stirred at room temperature for 1 h. The addition of an aqueous saturated solution of NH_4PF_6 (1 mL) immediately produced a dark-brownish precipitate, that was filtered on a frit, washed with water, and dried under vacuum. Yield: 95.39 % (98 mg, 0.101 mmol); ^{1}H NMR (500 MHz, [D$_6$]acetone, 25 °C): $\delta = 0.28$ (d, $^3J_{33ac,32} = 7.2$ Hz, 3H; H33a–c), 0.58 (d, $^3J_{37ac,32} = 6.9$ Hz, 3H; H37a–c), 1.18 (m, 1H; H32), 1.30 (d, $^3J_{35ac,34} = {}^3J_{36ac,34} = 1.4$ Hz, 6H; H36a–c, H35a–c), 2.17 (s, 3H; H38), 3.04 (m, 1H; H34), 3.15 (m, 1H; H20), 3.99 (dd, $^3J_{21b,20} = 8.3$ Hz, $^2J_{21b,21a} = 9.6$ Hz, 1H; H21b), 4.43 (dd, $^3J_{21a,20} = 2.5$ Hz, $^2J_{21a,21b} = 9.6$ Hz, 1H; H21a), 5.12–5.14 (m, 2H; H30b, H30a), 5.64 (m, 1H; H31), 7.09 (ddd, $^4J_{2,4} = 1.4$ Hz, $^3J_{2,3} = 5.8$ Hz, $^3J_{2,1} = 6.8$ Hz, 1H; H2), 7.31 (dd, $^4J_{24,26} = 0.9$ Hz, $^3J_{24,25}$ 7.9 Hz, 1H; H24), 7.60 (td, $^4J_{25,27} = 1.2$ Hz, $^3J_{25,24} = {}^3J_{25,26}$ 7.9 Hz, 1H; H25), 7.92 (m, 3H; H1, H26, H3), 8.00 (ddd, $^4J_{14,12} = 1.2$, $^3J_{14,15} = 5.8$, $^3J_{14,13} = 7.8$ Hz, 1H; H14), 8.21 (dd, $^4J_{27,25} = 1.2$ Hz, $^3J_{27,26} = 7.9$ Hz, 1H; H27), 8.28 (t, $^3J_{8,7} = {}^3J_{8,9} = 8.0$ Hz, 1H; H8) 8.43 (td, $^4J_{13,15} = 1.2$ Hz, $^3J_{13,14} = {}^3J_{13,12} = 7.8$ Hz, 1H; H13), 8.46 (d, $^3J_{4,3} = 7.7$ Hz, 1H; H4), 8.65 (dd, $^4J_{7,9} = 0.7$ Hz, $^3J_{7,8} = 8.0$ Hz, 1H; H7), 8.78 (dd, $^4J_{9,7} = 0.7$ Hz, $^3J_{9,8} = 8.0$ Hz, H9), 8.86 (d, $^3J_{12,13} = 7.8$ Hz, H12), 9.46 ppm (d, $^3J_{15,14} = 7.8$ Hz, 1H; H15); UV/Vis (CH_2Cl_2): $\lambda_{max} = 280$ ($\varepsilon = 19150$), 315 (18540), 327 (17340), 383 (5970), 412 (5980), 541 (4730 $dm^3 mol^{-1} cm^{-1}$), 567 nm^{-1} (sh); $E_{1/2}$ (CH_2Cl_2): 1.32 V versus SSCE; $E_{1/2}$ (CH_3CN): 1.22 V versus SSCE; elemental analysis calcd (%) for $C_{35}H_{40}N_5O_2RuP_2F_{12}$: C 43.54, N 8.70, H 3.97; found: C 43.63, N 8.63, H 4.09.

(R_cR_c,S_aR_a)/(S_cS_c,R_aS_a)-[Ru^{II}(trpy)(Phbox-R)(py)](PF$_6$)$_2$, (R_cR_c,S_aR_a)-5a/(S_cS_c,R_aS_a)-5b: A sample of neat pyridine (0.30 mL, 3.70 mmol) was added to (R_cR_c,S_aR_a)-**3a** or (S_cS_c,R_aS_a)-**3b** (0.125 mmol, 100 and 103 mg respectively) dissolved in an acetone/H_2O mixture (1:1 v/v, 40 mL). The resulting solution was magnetically stirred at room temperature for two days and then a saturated solution of KPF_6 (1.5 mL) was added. A solid appeared in the solution immediately and was filtered, washed with a small amount of cold water, and dried under vacuum. For (R_cR_c,S_aR_a)-**5a**·0.5H_2O, Yield: 36.5 % (45 mg, 0.046 mmol); ^{1}H NMR (200 MHz, [D$_6$]acetone, 25 °C): $\delta = 0.40$ (t, $^3J_{33,32} = 7.5$ Hz, 3H; H33a–c), 1.00 (m, 2H; H32a–b), 1.16 (pt, $^3J_{35,34} = 7.5$ Hz, 3H; H35a–c), 1.57 (m, 1H; H34a), 1.84 (m, 1H; H34b), 2.85 (m, 1H; H20), 4.03 (t, $^3J_{21b,21a} = {}^3J_{21b,20} = 8.5$ Hz, 1H; H21b), 4.31 (dd, $^3J_{21a,21b} = 8.5$ Hz, $^3J_{21a,20} = 2$ Hz, 1H; H21a), 4.94 (pt, $^3J_{30a,30b} = {}^3J_{30a,31} = 9$ Hz, 1H; H30a), 5.39 (pt, $^3J_{30b,30a} = {}^3J_{31,30a} = 9$ Hz, 2H; H30b, H31), 7.0–9.4 ppm (m, 20H; H1–H9, H12–H15, H24–H27, H36–40); UV/Vis (CH_2Cl_2): $\lambda_{max} = 276$ ($\varepsilon = 22429$), 318 (30269), 370 (sh), 475 (sh), 518 nm^{-1} (5162 $dm^3 mol^{-1} cm^{-1}$); $E_{1/2}$ (CH_3CN): 1.15 versus SSCE; elemental analysis calcd (%) for $C_{36}H_{36}N_6O_2RuP_2F_{12}$·1.5$H_2O$: C 43.91, N 8.53, H 3.79; found: C 43.95, N 8.60, H 3.68. For (S_cS_c,R_aS_a)-**5b**, Yield: 55 % (68 mg, 0.067 mmol); ^{1}H NMR (500 MHz, [D$_6$]acetone, 25 °C): $\delta =$ 0.28 (d, $^3J_{33ac,32} = 7.0$ Hz, 3H; H33a–c), 0.55 (d, $^3J_{37ac,32} = 7.0$ Hz, 3H; H37a–c), 1.02 (d, $^3J_{36ac,34} = 7.0$ Hz, 3H; H36a–c), 1.03(m, 1H; H32), 1.20 (d, $^3J_{35ac,34} = 6.5$ Hz, 3H; H35a–c), 3.14 (m, H; H20), 1.51 (m, 1H; H34), 3.92 (t, $^3J_{21b,20} = {}^2J_{21b,21a} = 9.5$ Hz, 1H; H21b), 4.39 (dd, $^3J_{21a,20} = 2$ Hz, $^2J_{21a,20b} = 9.5$ Hz, 1H; H21a), 5.07 (t, $^3J_{30b,31} = {}^2J_{30b,30a} = 4.5$ Hz, 1H; H30b), 5.20 (dd, $^3J_{30a,31} = 5$, $^2J_{30a,30b} = 9.5$ Hz, 1H; H30a), 5.40 (m, 1H; H31), 7.12–7.16 (m, 3H; H2, H39, H41), 7.33 (dd, $^4J_{24,26} = 0.9$ Hz, $^3J_{24,25} = 7.9$ Hz, 3H; H24), 7.65 (td, $^4J_{25,27} = 0.9$ Hz, $^3J_{25,24} = {}^3J_{25,26} = 7.9$ Hz, 3H; H25), 7.70 (t, $^3J_{40,39} = {}^3J_{40,41} = 8$ Hz, 1H; H40), 7.88 (d, $^3J_{38,39/42,41} = 8.0$ Hz, H38, H42), 7.92 (td, $J = {}^4J_{3,1} = 1.2$ Hz, $^3J_{3,2} = {}^3J_{3,4} = 7.9$ Hz, 1H; H3), 7.98–8.00 (m, 2H; H26, H14), 8.10 (dd, $^4J_{1,3} = 1.2$ Hz, $^3J_{1,2} = 7.9$ Hz, 1H; H1), 8.18–8.20 (m, 2H; H8, H27), 8.43–8.44 (m, 2H; H13, H4), 8.58 (d, $^3J_{7,8} = 8$ Hz, 1H; H7), 8.78 (d, $^3J_{9,8} = 8$ Hz, 1H; H9), 8.87 (d, $^3J_{12,13} = 8$ Hz, 1H; H12), 9.32 ppm (d, $^3J_{15,14} = 8$ Hz, 1H; H15); UV/Vis (CH_2Cl_2): $\lambda_{max} = 278$ ($\varepsilon =$ 26080), 318 (35425), 370 (sh), 470 (sh), 512 nm^{-1} (5690 $dm^3 mol^{-1} cm^{-1}$); $E_{1/2}$ (CH_3CN): 1.18 V versus SSCE; elemental analysis calcd (%) for $C_{38}H_{40}N_6O_2RuP_2F_{12}$: C 45.48, N 8.37, H 4.02; found: C 45.57, N 8.39, H 4.10.

(S_cS_c,R_aS_a)-[Ru^{II}(trpy)(Phbox-*i*Pr)(2-OH-py)](PF$_6$)$_2$, (S_cS_c,R_aS_a)-6b: A sample of the aquacomplex (S_cS_c,R_aS_a)-**3b** (41 mg, 0.062 mmol) was dissolved in acetone (18 mL) containing molecular-sieves (700 mg). Then, 2-hydroxypyridine (20.5 mg, 0.213 mmol) was added and the resulting mixture was heated at 45 °C for 10 h. Addition of ether immediately generated a reddish solid that was filtered on a frit, washed with ether, and dried under vacuum. Yield: 65.86 % (30 mg, 0.030 mmol); ^{1}H NMR (500 MHz, [D$_6$]acetone, 25 °C): $\delta = 0.67$ (d, $^3J_{33ac,32} = 6.8$ Hz, 3H; H33a–c), 0.70 (d, $^3J_{37ac,32} = 6.8$ Hz, 3H; H37a–c), 0.85 (d, $^3J_{36ac,34} = 7.0$ Hz, 3H; H36a–c), 1.17 (d, $^3J_{36ac,34} = 6.5$ Hz, 3H; H36a–c), 1.50(m, 1H; H32), 3.54–3.58(m, 2H; H34, H20), 3.91 (t, $^3J_{21b,20} = {}^2J_{21b,21a} = 6.9$ Hz, 1H; H21b), 4.13 (t, $^3J_{30b,31} = {}^2J_{30b,30a} = 9.3$ Hz, 1H; H30b), 4.35 (t, $^3J_{21a,20} = {}^2J_{21a,21b} = 6.9$ Hz, 1H; H21a), 4.54–4.58 (m, 2H; H30a, H31), 5.83 (t, $^3J_{26,25} = {}^3J_{26,27} = 7.5$ Hz, 1H; H26), 6.09 (d, $^3J_{38,39} = 7.0$ Hz, 1H; H38), 6.12 (d, $^3J_{27,26} = 7.5$ Hz, 1H; H27), 6.27 (d, $^3J_{24,25} = 7.5$ Hz, 1H; H24), 7.16 (t, $^3J_{39,38} = {}^3J_{39,40} = 7.0$ Hz, 1H; H39), 7.22 (t, $^3J_{25,24} = {}^3J_{25,26} = 7.5$ Hz, 1H; H25), 7.42 (t, $^3J_{8,7} = {}^3J_{8,9} = 7.7$ Hz, 1H; H8), 7.49 (t, $^3J_{40,39} = {}^3J_{40,41} = 7.0$ Hz, 1H; H40), 7.55 (d, $^3J_{41,40} = 7.0$, 1H; H41), 7.74 (d, $^3J_{7,8} = 7.7$ Hz, 1H; H7), 7.81 (m, 2H; H14, H2), 8.13 (t, $^3J_{3,2} = {}^3J_{3,4} = 8.4$ Hz, 1H; H3), 8.18 (t, $^3J_{13,12} = {}^3J_{13,14} = 7.7$ Hz, 1H; H13), 8.32 (d, $^3J_{9,8} = 7.7$ Hz, 1H; H9), 8.59 (d, $^3J_{12,13} = 7.7$ Hz, 1H; H12), 8.97 (d, $^3J_{1,2} = 4.9$ Hz, 1H; H1), 9.00 ppm (d, $^3J_{15,14} = 4.7$ Hz, 1H; H15); UV/Vis (CH_2Cl_2): $\lambda_{max} = 276$ ($\varepsilon = 26120$), 316 (30050), 377 (sh), 494 (3920 $dm^3 mol^{-1} cm^{-1}$), 534 nm^{-1} (sh); $E_{1/2}$ (CH_2Cl_2): 0.755 V versus SSCE; elemental analysis calcd (%) for $C_{38}H_{39}N_6O_3RuP_2F_{12}$: C 44.76, N 8.24, H 3.95; found: C 44.89, N 7.98, H 4.22.

Acknowledgements

This research has been financed by MCYT of Spain through the projects BQU2003–02884, BQU2002–04112-C02—02, and CTQ2004–01546/BQU. A.L., M.S., and M.G. are grateful to CIRIT Generalitat de Catalunya (Spain) for financial support, and A.L. for the aid SGR2001-UG-291. A.P., M.S., and M.D. thank the Centre de Supercomputació de Catalunya (CESCA) for partial funding of computer time. A.L. also thanks Johnson and Matthey for the loan of $RuCl_3$·xH_2O. E.P., X.S., and A.P. are grateful for the award of doctoral grants from CIRIT, UdG, and MEC, respectively.

[1] a) A. G. Lappin, R. A. Marusak, *Coord. Chem. Rev.* **1991**, *109*, 125–180; b) W. P. Griffith, *Chem. Soc. Rev.* **1992**, *21*, 179–185; c) J. Wing-Sze Hui, W-T. Wong, *Coord. Chem. Rev.* **1998**, *172*, 389–436; d) M. J. Clarke, *Coord. Chem. Rev.* **2002**, *232*, 69–93; e) T. J. Meyer, M. H. V. Huynh, *Inorg. Chem.* **2003**, *42*, 8140–8169.

[2] a) D. W. Thompson, J. R. Schoonover, D. K. Graff, C. N. Fleming, T. J. Meyer, *J. Photochem. Photobiol. A* **2000**, *137*, 131–134; b) H. E. Toma, R. M. Serrasqueiro, R. C. Rocha, G. J. F. Demets, H. Winnischofer, K. Araki, P. E. A. Ribeiro, C. L. Donnici, *J. Photochem. Photobiol. A* **2000**, *135*, 185–191; c) M. H. Keefe, K. D. Benkstein, H. T. Hupp, *Coord. Chem. Rev.* **2000**, *205*, 201–228; d) D. S. Tyson, C. R. Luman, X. Zhou, F. N. Castellano, *Inorg. Chem.* **2001**, *40*, 4063–4071; e) V. Valzani, A. Juris, *Coord. Chem. Rev.* **2001**, *211*, 97–115; f) D. M. Dattelbaum, C. M. Hartshorn, T. J. Meyer, *J. Am. Chem. Soc.* **2002**, *124*, 4938–4939; g) C. N. Fleming, L. M. Dupray, J. M. Papanikolas, T. J. Meyer, *J. Phys. Chem. A* **2002**, *106*, 2328–2334; h) R. Lomoth, T. Haupl, O. Jahansson, L. Hammarstrom, *Chem. Eur. J.* **2002**, *8*, 102–110.

[3] a) S. O. Kelly, J. K. Barton, *Science* **1999**, *283*, 375–381; b) D. B. Hall, R. E. Holmlin, J. K. Barton, *Nature* **1996**, *384*, 731–735; c) C. J. Burrows, J. G. Muller, *Chem. Rev.* **1998**, *98*, 1109–1152; d) G. B. Schuster, *Acc. Chem. Res.* **2000**, *33*, 253–260; e) S. C. Weatherly, I. V. Yang, H. H. Thorp, *J. Am. Chem. Soc.* **2001**, *123*, 1236–1237.

[4] a) S. I. Murahashi, H. Takaya, T. Naota, *Pure Appl. Chem.* **2002**, *74*, 19–24; b) T. Naota, H. Takaya, S.-I. Murahashi, *Chem. Rev.* **1998**, *98*, 2599–2660; c) M. Rodríguez, I. Romero, A. Llobet, A. Deronzier, M. Biner, T. Parella, H. Stoeckli-Evans, *Inorg. Chem.* **2001**, *40*,

4150–4156; d) U. J. Jauregui-Haza, M. Dessoudeix, Ph. Kalck, A. M. Wilhelm, H. Delmas, *Catal. Today* **2001**, *66*, 297–302.

[5] a) R. Ballardini, V. Balzani, A. Credi, M. T. Gandolfi, M. Venturi, *Int. J. Photoenergy* **2001**, *3*, 63–77; b) P. R. Ashton, R. Ballardini, V. Balzani, A. Credi, K. R. Dress, E. Ishow, C. J. Kleverlaan, O. Kocian, J. A. Preece, N. Spencer, J. F. Stoddart, M. Venturi, S. Wenger, *Chem. Eur. J.* **2000**, *6*, 3558–3574; c) E. Baranoff, J.-P. Collin, J. Furusho, Y. Furusho, A.-C. Laemmel, J.-P. Sauvage, *Inorg. Chem.* **2002**, *41*, 1215–1222; d) T. Kojima, T. Sakamoto, Y. Matsuda, *Inorg. Chem.* **2004**, *43*, 2243–2245.

[6] A. H. Velders, A. C. G. Hotze, J. G. Haasnoot, J. Reedijk, *Inorg. Chem.* **1999**, *38*, 2762–2763.

[7] a) E. Yashima, K. Maeda, Y. Okamoto, *Nature* **1999**, *399*, 449–451; b) L. J. Pins, J. Huskens, T. de Jong, P. Timmerman, D. N. Reinhoudt, *Nature* **1999**, *398*, 498–502; c) B. L. Feringa, R. A. van Delden, N. Komura, E. M. Geertsema, *Chem. Rev.* **2000**, *100*, 1789–1816; d) P. Hayoz, A. Von Zelewsky, H. Stoeckli-Evans, *J. Am. Chem. Soc.* **1993**, *115*, 5111–5114; e) A. Von Zelewsky, *Coord. Chem. Rev.* **1999**, *190–192*, 811–825; f) U. Knof, A. Von Zelewsky, *Angew. Chem.* **1999**, *111*, 312–333; *Angew. Chem. Int. Ed.* **1999**, *38*, 302–322; g) A. Von Zelewsky, O. Mamula, *J. Chem. Soc. Dalton Trans.* **2000**, 219–231; h) J. W. Canary, S. Zahn, *Trends Biotechnol.* **2001**, *19*, 251–255; i) J. Lacour, A. Londez, *J. Organomet. Chem.* **2002**, *643–644*, 392–403; j) P. D. Knight, P. Scott, *Coord. Chem. Rev.* **2003**, *242*, 125–142.

[8] A. von Zelewsky, *Stereochemistry of Coordination Compounds*, Wiley, Chichester, **1996**.

[9] a) D. S. Hesek, Y. Inoue, S. R. L. Everitt, H. Ishida, M. Kunieda, M. D. Drew, *Inorg. Chem.* **2000**, *39*, 317–324; b) D. Hesek, G. A. Hembury, M. D. Drew, S. Taniguchi, Y. Inoue, *J. Am. Chem. Soc.* **2000**, *122*, 10236–10237; c) R. A. Sheldon, *Chirotechnology*, Marcel Dekker, New York, **1993**.

[10] a) A. Llobet, *Inorg. Chim. Acta* **1994**, *221*, 125–131; b) I. Romero, M. Rodríguez, A. Llobet, M.-N. Collomb-Dunand-Sauthier, A. Deronzier, T. Parella, H. Stoeckli-Evans, *J. Chem. Soc. Dalton Trans.* **2000** 1689–1694; c) C. Sens, M. Rodríguez, I. Romero, A. Llobet, T. Parella, B. P. Sullivan, J. Benet-Buchholz, *Inorg. Chem.* **2003**, *42*, 2040–2048; d) M. Rodríguez, I. Romero, A. Llobet, C. Sens, A. Deronzier, *Electrochim. Acta* **2003**, *48*, 1047–1054; e) X. Sala, M. Rodríguez, I. Romero, A. Llobet, G. Gonzàlez, M. Martínez, J. Benet-Buchholz, *Inorg. Chem.* **2004**, *43*, 5403–5409; f) C. Sens, I. Romero, M. Rodríguez, A. Llobet, T. Parella, J. Benet-Buchholz, *J. Am. Chem. Soc.* **2004**, *126*, 7798–7799; g) X. Sala, A. Poater, I. Romero, M. Rodríguez, A. Llobet, X. Solans, T. Parella, T. M. Santos, *Eur. J. Inorg. Chem.* **2004**, *3*, 612–618.

[11] C. Bolm, K. Weickhardt, M. Zehnder, D. Glasmacher, *Chem. Ber.* **1991**, *124*, 1173–1180.

[12] A. El Hatimi, M. Gómez, S. Jansat, G. Muller, M. Font-Badía, X. Solans, *J. Chem. Soc. Dalton Trans.* **1998**, 4229–4236.

[13] a) A. Llobet, P. Doppelt, T. J. Meyer, *Inorg. Chem.* **1988**, *27*, 514–520; b) K. Barqawi, A. Llobet, T. J. Meyer, *J. Am. Chem. Soc.* **1988**, *110*, 7751–7759.

[14] F. Laurent, E. Plantalech, B. Donnadieu, A. Jiménez, F. Hernández, M. Martínez-Ripoll, M. Biner, A. Llobet, *Polyhedron* **1999**, *18*/25, 3321–3331.

[15] a) H. Kurosawa, H. Asano, Y. Miyaki, *Inorg. Chim. Acta* **1998**, *270*, 87–94; b) C. Sens, M. Rodríguez, I. Romero, A. Llobet, T. Parella, B. P. Sullivan, J. Benet-Buchholz, *Inorg. Chem.* **2003**, *42*, 8385–8394; c) L. F. Szczpura, S. M. Maricich, R. F. See, M. R. Churchill, K. J. Takeuchi, *Inorg. Chem.* **1995**, *34*, 4198–4205.

[16] M. Gómez, S. Jansat, G. Muller, M. A. Maestro, J. Mahia, *Organometallics* **2002**, *21*, 1077–1087.

[17] R. Cini, C. J. Pifferi, *J. Chem. Soc. Dalton Trans.* **1999**, 699–710.

[18] Standard deviations for the lengths and angles, $S_{n-1}=[(\Sigma_{i=1-n}\text{-}(CV-EV)^2)/(N-1)]^{1/2}$, where CV means calculated value, EV experimental value (X-ray data), and N is the number of bond lengths or angles taken into account (see Supporting Information for the list of bond lengths and angles considered in the calculation of S_{n-1} for complex (S_cS_c,R_aS_a)-**4b**).

[19] a) G. M. Sheldrick, SHELXS-97, Program for Crystal Structure Determination, *Acta Crystallogr.* **1990**, *A46*, 467–473; b) G. M. Sheldrick, SHELXL-97, Universität Göttingen, Göttingen, (Germany), **1997**.

[20] D. Flack, *Acta Crystallogr. Sect. A* **1983**, *39*, 876–881.

[21] a) E. J. Baerends, J. A. Autschbach, A. Bérces, C. Bo, P. M. Boerrigter, L. Cavallo, D. P. Chong, L. Deng, R. M. Dickson, D. E. Ellis, L. Fan, T. H. Fischer, C. Fonseca Guerra, S. J. A. van Gisbergen, J. A. Groeneveld, O. V. Gritsenko, M. Grüning, F. E. Harris, P. van den Hoek, H. Jacobsen, G. van Kessel, F. Kootstra, E. van Lenthe, V. P. Osinga, S. Patchkovskii, P. H. T. Philipsen, D. Post, C. C. Pye, W. Ravenek, P. Ros, P. R. T. Schipper, G. Schreckenbach, J. G. Snijders, M. Solà, M. Swart, D. Swerhone, G. te Velde, P. Vernooijs, L. Versluis, O. Visser, E. van Wezenbeek, G. Wiesenekker, S. K. Wolff, T. K. Woo, and T. Ziegler, ADF2002.03, Vrije Universiteit Amsterdam, Amsterdam, The Netherlands, **2000**; b) G. te Velde, F. M. Bickelhaupt, E. J. Baerends, C. Fonseca Guerra, S. J. A. Van Gisbergen, J. G. Snijders, T. Ziegler, *J. Comput. Chem.* **2001**, *22*, 931–967; c) E. J. Baerends, D. E. Ellis, P. Ros, *Chem. Phys.* **1973**, *2*, 41–51; d) E. J. Baerends, Ph.D. Thesis, Vrije Universiteit, Amsterdam, The Netherlands, **1975**; e) W. Ravenek, *Algorithms and Applications on Vector and Parallel Computers* (Eds.: H. J. J. te Riele, Th. J. Dekker, H. A. van de Vorst), Elsevier, Amsterdam, **1987**.

[22] G. te Velde, E. J. Baerends, *J. Comp. Physiol.* **1992**, *99*, 84–98.

[23] a) J. G. Snijders, E. J. Baerends, P. Vernooijs, *At. Nucl. Data Tables* **1982**, *26*, 483–509; b) P. Vernooijs, J. G. Snijders, E. J. Baerends, *Slater-Type Basis Functions for the Whole Periodic System. Internal Report*, Vrije Universiteit of Amsterdam, The Netherlands, **1981**.

[24] J. Krijn, E. J. Baerends, *Fit Functions in the HFS Method. Internal Report (in Dutch)*, Vrije Universiteit of Amsterdam, The Netherlands, **1984**.

[25] A. D. Becke, *Phys. Rev. A* **1988**, *38*, 3098–3100.

[26] J. P. Perdew, Y. Wang, *Phys. Rev. B* **1992**, *45*, 13244–13249.

[27] A. Klamt, G. Schüürmann, *J. Chem. Soc. Perkin Trans. 1* **1993**, 799–805.

[28] C. C. Pye, T. Ziegler, *Theor. Chem. Acc.* **1999**, *1101*, 396–408.

[29] Gaussian 98 (Revision A.11), M. J. Frisch, G. W. Trucks, H. B. Schlegel, G. E. Scuseria, M. A. Robb, J. R. Cheeseman, V. G. Zakrzewski, J. A. Montgomery, Jr., R. E. Stratmann, J. C. Burant, S. Dapprich, J. M. Millam, A. D. Daniels, K. N. Kudin, M. C. Strain, O. Farkas, J. Tomasi, V. Barone, M. Cossi, R. Cammi, B. Mennucci, C. Pomelli, C. Adamo, S. Clifford, J. Ochterski, G. A. Petersson, P. Y. Ayala, Q. Cui, K. Morokuma, P. Salvador, J. J. Dannenberg, D. K. Malick, A. D. Rabuck, K. Raghavachari, J. B. Foresman, J. Cioslowski, J. V. Ortiz, A. G. Baboul, B. B. Stefanov, G. Liu, A. Liashenko, P. Piskorz, I. Komaromi, R. Gomperts, R. L. Martin, D. J. Fox, T. Keith, M. A. Al-Laham, C. Y. Peng, A. Nanayakkara, M. Challacombe, P. M. W. Gill, B. Johnson, W. Chen, M. W. Wong, J. L. Andres, C. Gonzalez, M. Head-Gordon, E. S. Replogle, J. A. Pople, Gaussian, Inc., Pittsburgh PA, **2001**.

[30] D. R. Lide, *Handbook of Chemistry and Physics*, 83rd ed., CRC Press LLC, Boca Raton, London, **2002–2003**.

[31] D. M. Dolney, G. D. Hawkins, P. Winget, D. A. Liotard, C. J. Cramer, D. G. Truhlar, *J. Comput. Chem.* **2000**, *21*, 340–366.

[32] J. Kong, C. A. White, A. I. Krylov, C. D. Sherrill, R. D. Adamson, T. R. Furlani, M. S. Lee, A. M. Lee, S. R. Gwaltney, T. R. Adams, C. Ochsenfeld, A. T. B. Gilbert, G. S. Kedziora, V. A. Rassolov, D. R. Maurice, N. Nair, Y. Shao, N. A. Besley, P. E. Maslen, J. P. Dombroski, H. Daschel, W. Zhang, P. P. Korambath, J. Baker, E. F. C. Byrd, T. Van Voorhis, M. Oumi, S. Hirata, C.-P. Hsu, N. Ishikawa, J. Florian, A. Warshel, B. G. Johnson, P. M. W. Gill, M. Head-Gordon, J. A. Pople, *J. Comput. Chem.* **2000**, *21*, 1532–1548.

[33] B. P. Sullivan, J. M. Calvert, T. J. Meyer, *Inorg. Chem.* **1980**, *19*, 1404–1407.

Received: July 11, 2005
Published online: January 17, 2006

